

Ultrahigh-fidelity qubits for quantum computing

Mark G. Raizen,^{1,2,*} Shou-Pu Wan,^{1,2} Chuanwei Zhang,³ and Qian Niu²

¹Center for Nonlinear Dynamics, The University of Texas at Austin, Austin, Texas 78712, USA

²Department of Physics, The University of Texas at Austin, Austin, Texas 78712, USA

³Department of Physics and Astronomy, Washington State University, Pullman, Washington 99164, USA

(Received 9 June 2009; revised manuscript received 21 July 2009; published 28 September 2009)

We analyze a system of fermionic ⁶Li atoms in an optical trap and show that an atom “on demand” can be prepared with ultrahigh fidelity, exceeding 0.999 98. This process can be scaled to many sites in parallel, providing a realistic method to initialize N qubits at ultrahigh fidelity for quantum computing. We also show how efficient quantum gate operation can be implemented in this system and how spatially resolved single-atom detection can be performed.

DOI: 10.1103/PhysRevA.80.030302

PACS number(s): 03.67.Lx, 42.50.Dv, 42.50.Ex

The potential impact of quantum computing has stimulated a worldwide effort to develop the necessary experimental and theoretical resources [1,2]. The most challenging aspect of quantum computing is the requirement for ultrahigh fidelity in each step. The necessary starting point is initialization of a scalable number of qubits at ultrahigh fidelity. In this Rapid Communication, we consider a system of fermionic atoms and show that an atom “on demand” can be prepared in the ground state of a trap with fidelity exceeding 0.999 98, providing a realistic solution to the initialization problem in quantum computing. We discuss how that process can be scaled to many sites in parallel, enabling pairwise entanglement operations. Finally, we show how spatially resolved detection of each state can be implemented.

We first address the question of how to trap one atom on demand in the ground state of a trap. While this step has not yet been demonstrated experimentally, progress has been made for bosonic atoms using the method of laser culling [3–5]. One of the key questions is that of fidelity of the number state, and in that regard bosons are not ideal because they rely on strong interactions to maintain a relatively large excitation gap and to suppress low-frequency excitations during the culling process. This leads us to propose instead fermionic atoms, where a precise number is rigorously enforced by the Pauli exclusion principle. More specifically, we propose to use ⁶Li as the atom of choice. This atom has the advantage that the interaction strength and sign (attractive or repulsive) can be tuned with an external magnetic field. Two magnetic sublevels of one hyperfine ground state $|F=\frac{1}{2}, m_F=\frac{1}{2}\rangle$ and $|F=\frac{1}{2}, m_F=-\frac{1}{2}\rangle$ are used to define a qubit. We denote these states as $|\uparrow\rangle$ and $|\downarrow\rangle$, respectively. These states both become high-field seekers at large magnetic field with a well-defined frequency splitting that is nearly field independent, hence, insensitive to magnetic noise.

The starting point of the on demand single-atom preparation is laser-cooled ⁶Li atoms that are optically trapped in the two spin states [6,7]. The atoms can be cooled by evaporation at a magnetic field around 300 G, where the scattering length $a_s \approx -300a_0$ (a_0 is the Bohr radius). a_s is large enough for an efficient evaporation of the spin mixture and is also at

a minimum as a function of magnetic field, greatly reducing the effects of magnetic noise. After evaporative cooling, a weakly interacting degenerate Fermi gas forms at temperature $T \ll T_F$, where T_F is the Fermi temperature. The single-atom preparation process can be split into three steps:

Step I. The magnetic field is tuned to near ~ 0 G from the initial field of 300 G, resulting in a noninteracting degenerate Fermi gas (DFG). In this state, a spin pair fills each level, up to approximately the Fermi level.

Step II. Atom pairs are ejected by laser culling. This is accomplished by adiabatic lowering of the optical potential. This prepares a single pair in the ground state.

Step III. The well is adiabatically split into two parts that are spatially separated. In the presence of a magnetic field bias, this prepares one spin state on the left and the other on the right. Each atom can then serve as the initial state for a qubit.

With this method, an array of N microtraps would prepare $2N$ qubits. We now show in detail how ultrahigh fidelity is enforced at each step.

Step I. We first must justify the adiabaticity of this step. In the presence of a scattering length $a_s \approx -300a_0$ between the $|\uparrow\rangle$ and $|\downarrow\rangle$ states, the Fermi gas is weakly interacting. At $T=0$, the Fermi gas may form a BCS state. The pairing gap for such a state can be estimated through $\Delta \approx 0.5E_F \exp(\pi/2k_F a)$ [8]. For a degenerate ⁶Li gas with $k_F^{-1} \sim 1000a_0$, the pairing gap $\Delta \approx 0.002E_F$. For such a small pairing gap, finite temperature effects dominate, and there is actually no BCS pairing. However, the finite temperature does not affect the ground-state occupation probability. Consider a temperature $T=0.05T_F$, for which the ground-state occupation probability is approximately $1/[\exp(-E_F/k_B T)+1]=1-4 \times 10^{-5}$. Therefore, a fast sweep of the magnetic field (i.e., the scattering length) to the noninteracting region does not affect the ground-state occupation probability or the fidelity of the single-atom preparation.

Step II. A noninteracting DFG in a deep optical trap serves as the starting point for the laser culling process. We assume that the trapping frequencies in the two transverse directions are significantly higher than along the axis, and only the ground transverse state can be supported. We therefore limit our analysis to one spatial dimension. The trap wall is reduced to a level slightly below the ionization

*raizen@physics.utexas.edu

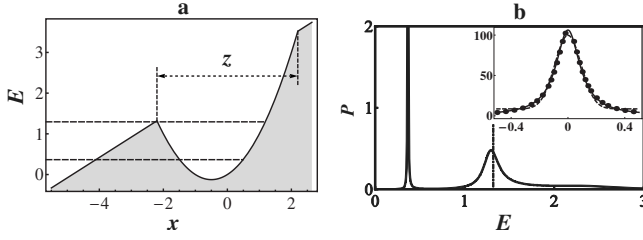


FIG. 1. The simulation model for laser culling in a one-dimensional optical trap. We take $x_0 \equiv \sqrt{\hbar/m\omega}$ as the unit of length (m is the mass of the ${}^6\text{Li}$ atom), $\hbar\omega$ as the unit of energy, and $\hbar\omega/x_0$ as the unit of force. (a) Truncated harmonic trap with magnetic gradient. The trapping potential for one state is shown. Parameters used to specify the trap: trap size z is the length of the parabolic portion in the potential profile; force f is the slope of the linear portion in the potential profile. Dashed lines denote the levels of the ground and first-excited states. (b) Plot of $P(E)$ as a measure of density of states of the quasibound states. Trap size $z=4.4$; force $f=0.5$. The vertical line (dot dashed) denotes the barrier height of the trap. Inset: zoomed-in view of the resonance peak of the ground quasibound state (dots) as shown in the main figure and Lorentzian (solid) and Gaussian (dashed) regressions. Horizontal axis is in units of $\gamma/2$, where γ is the full width at half maximum (FWHM) of the resonance peak.

threshold of the first-excited state of the optical dipole trap. The trap reduction rate is chosen to fulfill the adiabaticity requirement. To that end, we maintain a constant trapping frequency ω throughout the laser culling process, which can be accomplished by dynamically varying the focus of the beam [9]. (In practice, this step may not be necessary, but it greatly simplifies the calculation.) According to the Wentzel-Kramers-Brillouin (WKB) method, atoms with energy much lower than the trap depth are completely unaffected by the change in the depth of the trap. The adiabaticity condition is fulfilled as long as the WKB approximation is valid, which holds until the trap depth is around $3\hbar\omega/2$, where $\hbar \equiv h/2\pi$ and h is Planck's constant. Near and beyond this point, the trap reduction rate must be slowed down to maintain adiabaticity.

A constant force (or tilt) f is also needed to sweep the atoms away from the microtraps as soon as they are ionized, which is generated by applying a magnetic field gradient. For simplicity, we assume the force has a positive sign for state $|\uparrow\rangle$. In our simulation, we approximate the optical trap with a truncated harmonic potential [see Fig. 1(a)], which is specified by the trap size z . After reaching a minimum trap size z_m , the trap is held for a certain time to allow ionized atoms to escape, while keeping the ground-state atom pair with high probability. The trap depth, magnetic force, and holding time are adjusted to optimize fidelity. Finally, the trap wall (and size) is adiabatically raised to a higher level to preserve the resultant Fock state.

Our simulation method is described below. We assume that the ground-state fidelity is unchanged until the ionization energy of the first-excited state is approached. Because of the tilt, the trap has no stationary bound state, only quasibound states, which, as $z \rightarrow \infty$, become the bound states. The lifetimes of the quasibound states determine the rate of the change in the trap occupation probability. The optimized

final trap depth, tilt, and holding time is calculated based on the details explain below.

Suppose a stream of incoming atoms is incident from $x=-\infty$, with energy E , scattered by the trap potential. Let $\psi_E(x)$ be the wave function of the stationary state of the incoming atoms, which is assumed to have unit amplitude at $x=-\infty$. We assume the trap is located at $[-z/2, z/2]$. Outside the trap ($x < -z/2$), $\psi_E(x)$ is a superposition of Airy functions $\text{Ai}(x)$ and $\text{Bi}(x)$ with necessary superposition amplitudes and phases; inside the trap,

$$\psi_E(x) = a(E)e^{-x^2/2}H_\nu(x), \quad (1)$$

where $H_\nu(x)$ is the Hermite function of degree ν , $a(E)$ is the amplitude. We require $\psi_E(x)$ be continuous and differentiable for all ϵ , by which $a(E)$ is obtained. Of special interest to us are those states that have significant amplitude in the trap area because they correspond to the quasibound states of the trap. We define $P(E) \equiv |a(E)|^2$. For simplicity, we can take $P(E)$ as a measure of the density of states of the trap. We plot $P(E)$ in Fig. 1(b). Note that in the limit of zero magnetic force, the peaks at $E \approx 0.366$ and 1.29 correspond to the ground and first-excited states of the truncated harmonic trap, respectively.

$P(E)$ describes not only the ionization thresholds but also the dynamical properties of the quasibound states. To see that, we study the evolution of a wave function $\phi(x, t)$. Imagine that at time $t=0$, we have

$$\phi(x, 0) = \begin{cases} c\psi_{E_0}(x) & -z/2 < x < z/2 \\ 0 & \text{otherwise,} \end{cases} \quad (2)$$

where E_0 is one of the resonance energies, c is a normalization factor such that $\int_{-\infty}^{\infty} |\phi(x, 0)|^2 dx = 1$ and there is no other atom source. Subsequently, the atom will start to tunnel out of the trap. The probability $R_{E_0}(t)$ for an atom to remain in the trap is given by $\int_{-z/2}^{z/2} dx |\phi(x, t)|^2$. To evaluate $R_{E_0}(t)$, we expand $\phi(x, t)$ in terms of the wave functions of the stationary states $\psi_E(x)$. Note that in the vicinity of a resonance peak at $E=E_0$, one can write the wave function $\psi_E(x) \approx C(E)a(E)\psi_{E_0}(x)$, where $C(E)$ is a slowly varying quantity. Also

$$\int_{-z/2}^{z/2} dx \psi_E^*(x)\psi_{E_0}(x) \approx \int_{-\infty}^{\infty} dx \psi_E^*(x)\psi_{E_0}(x) \quad (3)$$

for $E \neq E_0$, due to the oscillatory nature of Airy functions. We find

$$R_{E_0}(t) \approx |C(E_0)|^2 \left| \int_{E_0-\epsilon/2}^{E_0+\epsilon/2} P(E)e^{iEt} dE \right|^2, \quad (4)$$

where ϵ is the range of integration. In the vicinity of a resonance peak, the function $P(E)$ is essentially Lorentzian [see inset of Fig. 1(b)], and we finally obtain

$$R_{E_0}(t) \approx e^{-\gamma_{E_0} t}, \quad (5)$$

where γ_{E_0} is the FWHM of the resonance peak at $E=E_0$. The lifetime of the quasibound state at $E=E_0$ is $\tau_{E_0} = \gamma_{E_0}^{-1}$. Equation (5) is used to determine an optimized combination of

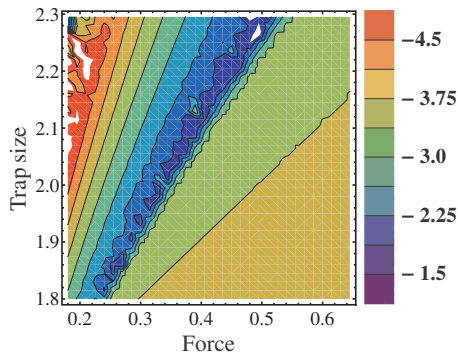


FIG. 2. (Color) Ground-state fidelity after laser culling. A varying holding time is allowed to ensure that the residual probability for atoms in excited quasibound states is no larger than 10^{-5} . Shown in the panel is the base-10 logarithm of the ground-state fidelity loss. Red (blue) color represents high (low) fidelity. The white areas are out-of-range clippings: near the left-hand side, the white areas should be redder than its surrounding color; near center top, the white area should be bluer than its surrounding color.

minimum trap depth, magnetic force, and holding time for the best fidelity. It is also worth noting that ultimately the *difference* in the lifetimes between the ground and the first-excited quasibound states determines the fidelity of producing a pair of atoms in the ground state of the trap.

Taking into account all the steps in laser culling, we show the fidelity of preparing a single pair of atoms in the ground state of a microtrap in Fig. 2. Choosing culling parameters near the upper-left corner of the figure results in ultrahigh fidelity. For a set of realistic parameters: trapping frequency $\omega=2\pi\times 1$ kHz, magnetic field gradient 0.66 G/cm, and truncated trap size $8.8\ \mu\text{m}$, the ground-state to first-excited-state lifetime ratio is 7.53×10^5 . With a holding time of 218 ms, we get a residual probability of 10^{-5} for the excited-state and a ground-state occupation probability larger than 0.999 98.

Step III. Finally, the pair of atoms are split and trapped in the ground state of two adjacent microtraps. In order to achieve deterministic splitting, where one spin state is driven to the left and the other to the right, we impose a magnetic field gradient (providing a force f) while we adiabatically split the optical tweezer (that holds the pair) into two beams [10]. With an appropriate magnetic field gradient and a separating barrier, this step can be realized at ultrahigh fidelity. Since $|\downarrow\rangle$ is a low-field seeker and $|\uparrow\rangle$ is a high-field seeker at low magnetic field, each atom is displaced to a different location as soon as the trap is split.

We adopt a simpler potential than that of a realistic optical tweezer. The trap is composed of two spliced sections of parabolic trap with identical trapping frequency ω , each of which has an energy minimum located at $\pm d/2$, respectively, where d is the separation distance. We numerically calculate the eigenenergy levels and wave functions of such a double-well structure in the parameter space of f and d . One needs to choose a path in the parameter space such that a sufficient gap between the ground and first-excited states is maintained throughout the splitting process in order to suppress transitions from the ground state. With a trapping frequency

$\omega=2\pi\times 1$ kHz, a magnetic field gradient of 0.66 G/cm and a separation displacement $d=6.25\ \mu\text{m}$, we find 0.999 98 splitting fidelity.

So far, we have shown that two initialized fiducial states can be prepared at ultrahigh fidelity. How can one scale this process to multiple sites and make the “switchyard” of multiplexed beams to perform the required complex operations? The scalability of this system can be achieved using scalable microelectromechanical systems (MEMS) technology [11]. Using this technology, an array of beams can be directed to each site, where individual atoms can be trapped. An alternative approach was developed in Ref. [12]. By steering the beams, one can transport individual atoms and bring them into pairwise interaction with arbitrary control. An array of microtraps would most easily be accomplished with red-detuned beams that create attractive potentials along the axis. This technique also enables the creation of a two-dimensional optical trap array and entanglement of any pair using the qubit transfer technique of Ref. [10]. This could extend the linear case, where only nearest-neighbor operations are possible.

We now consider single-qubit gates and two-qubit gates in this system. The implementation of a single-qubit gate requires the capability to address each atom individually. This can be accomplished with stimulated Raman transitions, as is currently employed with trapped ions [13,14] and with neutral atoms [15]. The realization of a two-qubit gate can be based on collisions between bosonic atoms [16]. This scheme was realized experimentally with atoms in an optical lattice [17]. Fermionic atoms in the same internal state cannot collide due to the Pauli exclusion principle. However, atoms in different states can have a large collisional shift, which can be used to engineer two-qubit SWAP (or $\sqrt{\text{SWAP}}$) gates, as proposed in Ref. [18]. The scattering length can be made very large by tuning closer to the Feshbach resonance. For a set of parameters $\omega=2\pi\times 1$ kHz and $a_s\sim 330a_0$, a high-fidelity $\sqrt{\text{SWAP}}$ gate can be implemented in a time period of about 40 ms. We envision that with an array of many qubits, a sequence of $\sqrt{\text{SWAP}}$ operations can build scalable entanglement in this system. This two-qubit operation, together with single-qubit rotations, provides a set of universal quantum gates.

The detection of each qubit state at the end of a quantum computation can be accomplished by a spatially resolved fluorescent imaging [19,20]. This stage must also resolve the spin of each location. This can be accomplished with the same method that was used to separate the spin pair followed by fluorescent imaging.

It is important to consider possible technical limitations on the fidelity. The only coupling to the environment is through collisions with background gas and the interaction with the optical tweezers. The first limitation can be overcome with better vacuum and is not fundamental. The optical tweezers can cause heating due to light scattering, intensity noise, and pointing fluctuations. These effects have all been studied in detail in Ref. [21]. The heating rate of atoms in a CO_2 optical tweezer is extremely small. For a well depth of 0.4 mK, the scattering time is 3400 s for one photon per atom. The heating rate due to intensity noise is $2\ \mu\text{K/s}$, and the heating rate due to pointing fluctuations is $46\ \text{nK/s}$. In

our case, the well depth is at least $100\times$ smaller, so the corresponding effects are reduced by that factor. A CO_2 laser can be used for trapping in two transverse directions, where the trap depth must be higher. This would confine the atoms along a line. However, the optical tweezers that implement logic gates must be at a shorter wavelength in order to have sufficient spatial resolution. The trap depth in this direction need only be enough to contain the ground state, so we estimate that light scattering will not limit the quoted fidelity. Regarding intensity noise and optical pointing instability in the visible regime, these can be tightly controlled with active feedback loops. An extreme example of such control is the

LIGO project [22], where intensity noise is reduced to a fractional level of 10^{-8} over the relevant spectral band. We therefore conclude that the technical noise is not a fundamental limitation to the proposed fidelity.

We thank Jungsang Kim for helpful discussions about MEMS technology and thank Rob Clark for insightful comments on the manuscript. M.G.R. was supported by the NSF, the R.A. Welch Foundation under Grant No. F-1258, and the Sid W. Richardson Foundation. C.Z. was supported by WSU Startup fund and the ARO. Q.N. was supported by the NSF, the DOE, and the R.A. Welch Foundation under Grant No. F-1255.

-
- [1] G. Chen *et al.*, *Quantum Computing Devices: Principles, Designs, and Analysis* (CRC Press, Boca Raton, 2006).
- [2] M. A. Nielsen and I. L. Chuang, *Quantum Computation and Quantum Information* (Cambridge University Press, Cambridge, England, 2000).
- [3] A. M. Dudarev, M. G. Raizen, and Q. Niu, Phys. Rev. Lett. **98**, 063001 (2007).
- [4] C.-S. Chuu *et al.*, Phys. Rev. Lett. **95**, 260403 (2005).
- [5] M. Pons, A. del Campo, J. G. Muga, and M. G. Raizen, Phys. Rev. A **79**, 033629 (2009).
- [6] E. R. I. Abraham *et al.*, Phys. Rev. A **53**, R3713 (1996).
- [7] K. M. O'Hara, M. E. Gehm, S. R. Granade, S. Bali, and J. E. Thomas, Phys. Rev. Lett. **85**, 2092 (2000).
- [8] S. Giorgini, L. P. Piteavskii, and S. Stringari, Rev. Mod. Phys. **80**, 1215 (2008).
- [9] T. Kinoshita, T. R. Wenger, and D. S. Weiss, Phys. Rev. A **71**, 011602(R) (2005).
- [10] J. Beugnon *et al.*, Nat. Phys. **3**, 696 (2007).
- [11] C. Knoernschild *et al.*, Opt. Express **17**, 7233 (2009).
- [12] R. Dumke *et al.*, Phys. Rev. Lett. **89**, 097903 (2002).
- [13] R. Blatt and D. Wineland, Nature (London) **453**, 1008 (2008).
- [14] D. L. Moehring *et al.*, Nature (London) **449**, 68 (2007).
- [15] D. D. Yavuz *et al.*, Phys. Rev. Lett. **96**, 063001 (2006).
- [16] D. Jaksch, H. J. Briegel, J. I. Cirac, C. W. Gardiner, and P. Zoller, Phys. Rev. Lett. **82**, 1975 (1999).
- [17] O. Mandel *et al.*, Nature (London) **425**, 937 (2003).
- [18] D. Hayes, P. S. Julienne, and I. H. Deutsch, Phys. Rev. Lett. **98**, 070501 (2007).
- [19] M. Karski *et al.*, Phys. Rev. Lett. **102**, 053001 (2009).
- [20] K. D. Nelson, X. Li, and D. S. Weiss, Nat. Phys. **3**, 556 (2007).
- [21] K. M. O'Hara *et al.*, Phys. Rev. Lett. **82**, 4204 (1999).
- [22] F. Nocera, Class. Quantum Grav. **21**, S481 (2004).